TRENDS IN SCIENCES 2025; 22(9): 10225
https://doi.org/10.48048/tis.2025.10225
RESEARCH ARTICLE

Intercalation of Rhodamine B Dye into Zinc-Aluminum Layered Double Hydroxides: Structural, Textural, and Morphological Insights

Nursyafiqah Jori Roslan[1], Nur Nadia Dzulkifli[1], Tengku Shafazila Tengku Saharuddin[2], Hamizah Mohd Zaki[3], Syawal Mohd Yusof[4] and Sheikh Ahmad Izaddin Sheikh Ahmad Ghazali[1,*]

[1]Material, Inorganic and Oleochemistry (MaterInoleo) Research Group, School of Chemistry and Environment, Faculty of Applied Sciences, Universiti Teknologi MARA Negeri Sembilan Kampus Kuala Pilah, Negeri Sembilan 72000, Malaysia
[2]Industrial Chemical Technology Programme, Faculty of Science & Technology, Universiti Sains Islam Malaysia (USIM), Negeri Sembilan 71800, Malaysia
[3]Faculty of Applied Sciences, Universiti Teknologi MARA, Selangor 40450, Malaysia
[4]Faculty of Science and Technology, Universiti Kebangsaan Malaysia, Selangor 43600, Malaysia

([*]Corresponding author's e-mail: sheikhahmadizaddin@uitm.edu.my)

Received: 21 March 2025, Revised: 23 May 2025, Accepted: 1 June 2025, Published: 5 July 2025

Abstract

This research reports of Zinc-Aluminium layered double hydroxide material (ZAL) intercalated with the organic dye rhodamine b (ZARB) through a co-precipitation technique. The intercalation of ZAL with rhodamine b (RB) was conducted at various concentrations of rhodamine b ranging from 0.025 to 0.6 M, at a pH of 7.0 ± 0.5, and with an aging time of 18 h. ZAL and ZARB were characterized using PXRD, FTIR-ATR, BET, and SEM-EDX to confirm the intercalation of guest ions into the interlayer of the lamellar structure. The overall PXRD pattern of ZAL and the optimal concentration of ZARB at 0.2 M demonstrated an expansion of basal spacing from 8.9 to 11.0 Å, indicating successful intercalation of the ZAL compound with RB. The FTIR-ATR spectrum of ZAL and ZARB at 0.2 M exhibited peaks at 3,375 cm^{-1} (O-H), 1,617 cm^{-1} (C=C), 1,097 cm^{-1} (C-O), 758 and 608 cm^{-1} (Zn-OH and Al-OH), while small peaks at 1,334 cm^{-1} (N-O) indicated that RB was intercalated between the layered structure. The spatial orientation of ZARB at 0.2 M exhibited an interlayer region value of 6.19 Å for the ZAL nanocomposites. BET analysis revealed that ZAL and ZARB exhibited Type IV nitrogen adsorption-desorption isotherms with H1 hysteresis loops. ZAL surface area was 5.19 m^2g^{-1}, BJH desorption pore volume is 0.0238 cm^3g^{-1} and BJH average pore diameter is 18.05 nm. Upon modification with RB, ZARB surface area increased to 14.30 m^2g^{-1}, BJH desorption pore volume to 0.0538 cm^3g^{-1} and BJH average pore diameter is 20.27 nm. SEM-EDX morphology of ZAL revealed aggregated hexagonal plate-like with non-uniform sizes and shapes. Upon intercalation with RB into the layered double hydroxide, the structure formed flaky plate-like particles with a higher surface area. These results demonstrate the effective intercalation of RB into the ZAL framework, resulting in a nanocomposite with modified structural and morphological properties.

Keywords: Layered double hydroxide, Rhodamine B, Intercalation, Zinc-aluminum layered double hydroxide, Co-precipitation method

Introduction

Layered double hydroxides (LDHs) also known as hydrotalcite-like compound are a class of anionic clay materials. It has a unique structure comprising positively charged metal hydroxide layers and interlayer anions [1]. The most studies LDHs material are zinc-aluminum layered double hydroxide (ZAL) due to its high stability,

tunable composition and versatile capabilities of anion exchange [2,3] The basic structure of ZAL is represented by the formula $[Zn_1\text{-}xAl_x(OH)_2]^{(x+2)}[A^{n-}]_x \cdot yH_2O$, where x is classified as the molar ratio of aluminum to zinc, and A^{n-} is the interlayer anion. Due to this unique structure that allows intercalation of various molecules or ions, ZAL is an excellent LDH material for a wide range of applications such as catalysis, drug delivery, environmental remediation and sensing [4-6].

In recent times, intercalation of organic dyes such as rhodamine B with zinc aluminum layered double hydroxide (ZARB) has gained interest owning to their significant potential for developing advanced materials for sensing and environmental applications. Rhodamine B (RB) is generally utilized as a fluorescent dye that is toxic and persistent in the environment, making its removal or immobilization a critical challenge [7]. The intercalation of RB into ZAL is a promising strategy for encapsulating this dye within the LDH structure, thus preventing its leaching. The formation of ZARB enhances stability and facilitates its removal from aqueous environments.

This research demonstrates significant potential in advancing the fields of sensing and environmental technologies by providing insights into the intercalation process, enhancing the physicochemical properties of ZARB material, and paving the way for the development of innovative nanocomposites tailored for specific applications.

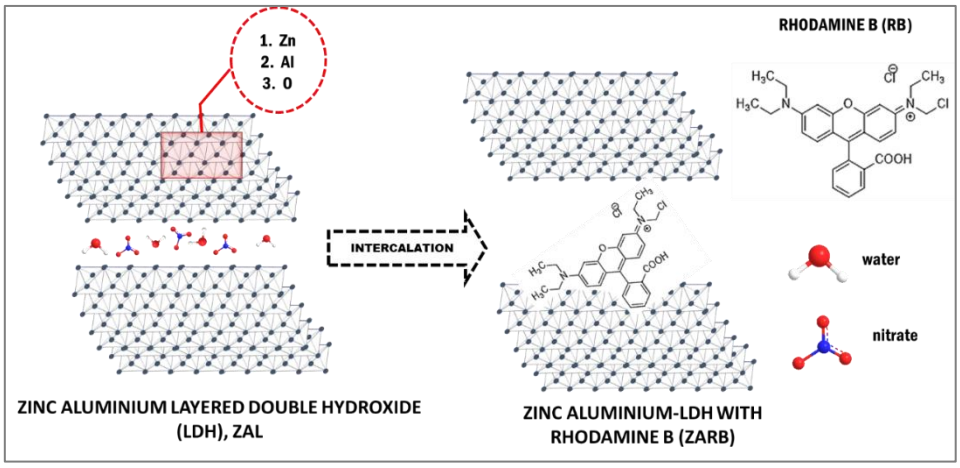

Figure 1 Intercalation of zinc aluminum LDH with rhodamine b.

Materials

The reagents used in the synthesis of zinc-aluminum LDH with rhodamine b (ZARB) were utilized without further purification. The reagents included zinc nitrate hexahydrate, ($Zn(NO_3)_2.6H_2O$, 98%, R&M Chemicals), Aluminum nitrate nonahydrate, ($Al(NO_3)_3.9H_2O$, 98.5%, R&M Chemicals), hydrochloric acid (HCl, 37%, R&M Chemicals), sodium hydroxide, (NaOH, 99%, Merck), rhodamine b (Macklin Chemicals). Standard nitrogen gas, 50 L.

Instrumentations

X-ray powder diffraction (PXRD) patterns were recorded at the 5° - 70° range using a Bruker D8 Advance PXRD diffractometer, operating under Cu Kα radiation at 40 kV (λ = 1.54059 Å) with scanning step at 0.01°. The Fourier transform infrared-attenuated total reflectance (FTIR-ATR) spectra were gained by Perkin Elmer Spectrum 100 mode in 4,000 - 400 cm^{-1}. The surface morphology of the materials was observed utilizing SEM, Supra 55 P. The textural properties (BET) of the materials were characterized by nitrogen physisorption analysis at −196 °C using a Micromeritics ASAP 2020 analyzer.

Methodology

Synthesis of Rhodamine B with Zinc Aluminum-Layered Double Hydroxide (ZARB) via co-precipitation method

The synthesis of ZARB was carried out via a direct co-precipitation method [8]. The 0.1 M of $Zn(NO_3)_2.6H_2O$ was mixed with 0.05 M of $Al(NO_3)_3.9H_2O$ in a aqueous solution 100 mL as, respectively, the mixture was then purged continuously

with nitrogen gas. The 0.2 M of RB anion was dissolved in 25 mL of deionized water and was added to mixture solution. The alkaline and acid solution (2.0 M NaOH and 1.0 M HCl) was added into the solution with intense stirring until the pH reached 7.5. The obtained slurry was aged for 18 h in an oil bath shaker at 65 °C. The red-pink slurry was centrifuged for 5 min at 3,500 rpm and washed with deionized water several times until excess nitrate and other impurities fully removed. The precipitate dried for 72 h at 80 °C. The generated nanocomposites were ground into by mortar and pestle until small size and used for further characterizations.

Results and discussion

X-ray powder diffraction (PXRD)

Figure 2 illustrates the PXRD patterns of ZAL, pure RB and its nanocomposites, ZARB at various concentrations in the range of 0.025 - 0.6 M. The diffractogram of ZAL exhibits high crystallinity and harmonious peaks at 2θ angles of 9.9° and 19.9°, which correspond to typical LDH with basal spacing of 8.9 Å. These peaks belong to nitrate peak as counter anion [9]. When 0.025 and 0.05 M concentrations of RB were introduced to ZAL, it resulting the nanocomposites at concentration 0.025 and 0.05 M show basal spacing of 8.8 and 8.9 Å, respectively, with no expansion of the basal spacing. This suggest that RB anion did not intercalate during the reaction and nitrate ions remained in the interlayer region of ZAL. Moreover, peaks at around 2θ angle = 30° - 39° for ZAL and all nanocomposites represent carbonate contamination, which is caused by interference of atmospheric carbon dioxide during the purging process of nitrogen gas [10].

Further, as concentration of RB anion increased to 0.1, 0.2, and 0.6 M, the diffraction peaks of ZARB nanocomposites show high crystallinity at 2θ angle = 8.3°, 8.0° and 8.2° of basal spacing 10.5, 11.0 and 10.7 Å, respectively. In the (003) plane, the (006) and (009) planes of ZAL shifted to lower angles upon successful intercalation [11]. The increasing of basal spacing due to the inclusion of new guest anion of RB into ZAL interlamellar, a number of peaks which are characteristics of RB anion phase were detected which contributed to the RB anion adsorbed onto the surface of ZAL due to the saturation of RB solution in the ZAL. However, based on the result exhibit the phase pure, well-ordered nanocomposites was obtained when ZAL synthesized with 0.2 M with increasing of basal spacing from

8.9 to 11.0 Å. These results exhibit excellent intercalation of RB anion at concentration 0.2 M into the interlayer of ZAL structure.

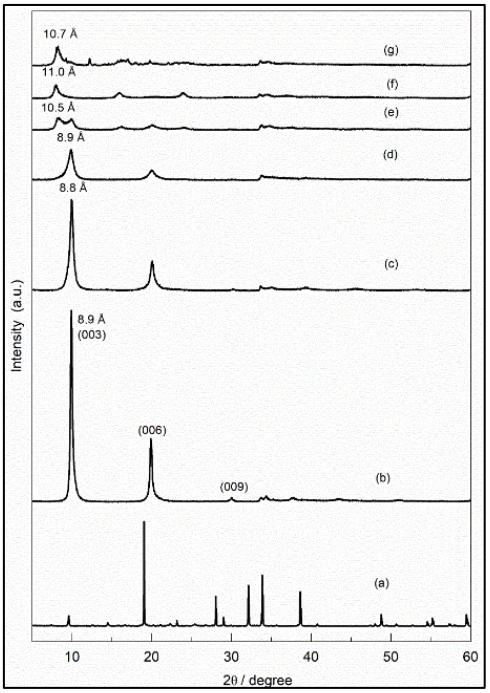

Figure 2 PXRD patterns of (a) pure RB, (b) ZAL, (c) ZARB (concentration 0.025 M), (d) ZARB (concentration 0.05 M), (e) ZARB (concentration 0.1 M), (f) ZARB (concentration 0.2 M), (g) ZARB (concentration 0.6 M).

Fourier transform infrared-attenuated total reflectance spectroscopy (FTIR-ATR)

Figure 3 shows the FTIR-ATR spectra of ZAL, pure RB and its nanocomposites, ZARB at various concentration in the range of 0.025 - 0.6 M. Based on the broad absorption peak in the ZAL at 3,395 cm^{-1}, the peak is denoted by the stretching vibration of O-H functional group caused by the adsorbed interlayer water of the hydroxyl of the layered structure. In addition, the small peak at 1,638 cm^{-1} corresponds to the deformation of water molecules, followed by the strong peak of nitrate, which occupies the counter anion at 1,348 cm^{-1}. The nanocomposite of ZARB at concentrations of 0.025 and 0.05 M exhibits broad absorption around 3,321 and 3,302 cm^{-1} dominated by the O-H stretching vibration of the adsorbed interlayer water. The weak bands at 1,634 and 1,638 cm^{-1} can be assigned to the bending of water in the interlayer. It should be highlighted that both nanocomposites possessed small intensity nitrate peaks at 1,360 and 1,363 cm^{-1}, indicating that the interlayer region is accommodated by nitrate ion as the guest. Thus, it is possible that THE intercalation of RB anion did not occur, which is consistent with the PXRD analysis in **Figure 2**.

The ZARB at concentration of 0.1, 0.2, and 0.6 M exhibit, the broadband centered at 3,382, 3,375 and 3,328 cm^{-1} which corresponds to the O-H stretching vibration of water molecules in the interlamellar region. Meanwhile, peaks at 1,638, 1,649 and 1,617 cm^{-1} belongs to C=C stretching vibration in aromatic rings of pure rhodamine, respectively. Furthermore, the significant peak of nanocomposites is newly formed as a sharp peak at 1,105, 1,097 and 1,102 cm^{-1} for RB concentrations of 0.1, 0.2 and 0.6 M, respectively. These peaks are characteristic of RB, corresponding to the C-O stretching vibration associated with carboxyl group (COOH). The peaks in the range of 548 and 788 cm^{-1} are attributed to Zn-OH and Al-OH. These results are in agreement with the PXRD analysis which is ZARB at concentration 0.2 M is the optimum concentration due to the presence of RB fingerprint in the interlayer of ZAL.

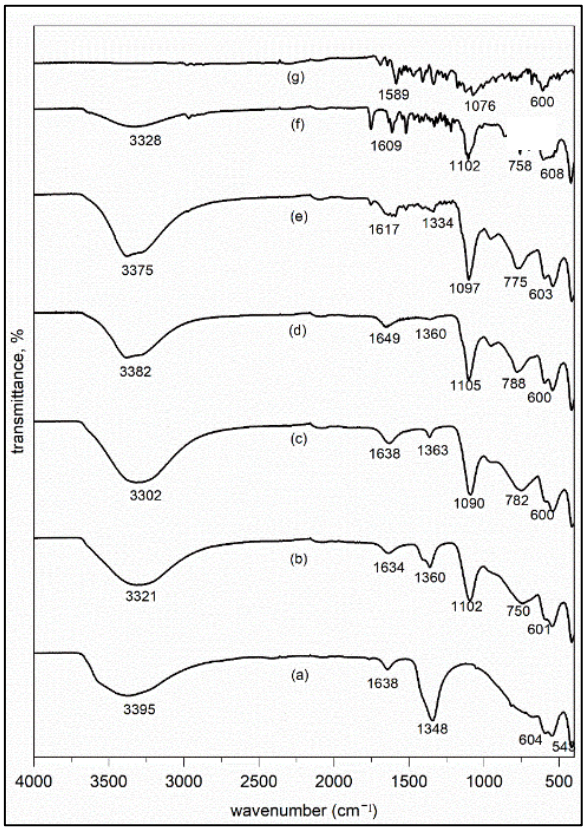

Figure 3 FTIR-ATR spectra of (a) ZAL, (b) ZARB (concentration 0.025 M), (c) ZARB (concentration 0.05 M), (d) ZARB (concentration 0.1 M), (e) ZARB (concentration 0.2 M), (f) ZARB (concentration 0.6 M), (g) pure RB.

Table 1 FTIR main absorption bands of ZAL and ZARB at concentration 0.025 to 0.6 M.

Absorption bands (cm^{-1})	Functional group
3302 - 3395	Stretching vibration of O-H
1638 (ZAL)	Bending vibration of O-H in water
1589 - 1649 (ZARB & pure RB)	C = C stretching vibration in aromatic rings
1334 - 1363	Stretching vibration of NO_3
1102 - 1097	C-O stretching vibration associated with carboxyl group (COOH)
548 - 788	Vibration of Zn-OH and Al-OH

Spatial orientation modelling

The three-dimensional molecular size of RB anion and its theoretical spatial orientation is shown in **Figure 4**. The structural arrangement was analyzed using ChemDraw 3D Pro software. The results of the PXRD and FTIR-ATR analyses are shown in **Figures 2** and **3**, respectively. The optimum concentration for intercalating RB with ZAL at 0.2 M is 11.0 Å. Therefore, the thickness of ZAL is 4.81 Å [12], the interlayer region of ZARB can be obtained by subtracting the total basal spacing of ZARB, the value is 6.19 Å. The values of interlayer region explained the area allocated for the spatial orientation of RB anion as they transferred into the intergalleries ZAL. The molecular size of RB anion can be determined by using crystallite size of ZARB from PXRD data, where the long axis, short axis and molecular thickness of RB anion structure were estimated 5.45, 3.93 and 5.45 Å, respectively. A theoretical orientation of RB anions seems likely to be oriented in a vertical manner adjacent to the positively charged brucite layer of ZAL. Thus, the value obtained for the interlayer ZAL is consistent with the enlargement of ZARB after RB anion has intercalated into layered structure.

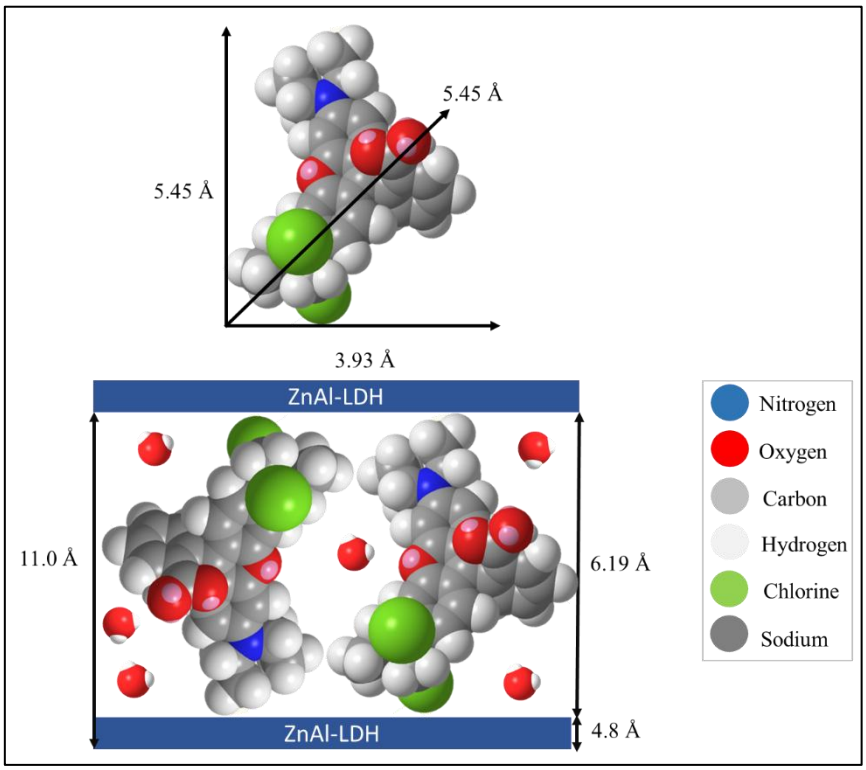

Figure 4 Molecular structural models of intercalated ZARB between ZAL interlayers.

Brunauer-teller- emmett (BET)

Intercalation of guest anion RB has a significant effect on the surface characteristics of ZAL and the formation of ZARB, as indicated by their textural properties (**Table 2**). With an average pore diameter of 18.05 nm, a BJH pore volume of 0.0238 cm^3/g, and a surface area of 5.19 m^2/g, ZAL shows limited porosity. Owning to the close stacking of LDH layer, this points to a compact, ordered layered structure with limited pore accessibility. On the other hand, ZARB shows an improvement of textural by increasing the average pore diameter of 20.27 nm, pore volume of 0.0538 cm^3/g, and surface area of 14.30 m^2/g. The increasing of pore volume and surface area exhibit that RB anion was successfully intercalated into ZAL, increasing the interlayer gap, decreasing aggregation, and generating more porosity. These results are in agreement with the structural data, as shown in **Figure 6**.

Both ZAL and ZARB display Type IV nitrogen adsorption-desorption isotherms with H1 hysteresis loops, suggesting uniform pores on mesoporous structure. ZAL with low surface area and pore volume, which express limited mesoporosity. The ZAL are compatible with the isotherm reduced nitrogen uptake. Meanwhile, ZARB at concentration 0.2 are reflected in isotherm with more noticeable hysteresis loop and increased nitrogen uptake resulting enhance the textural properties of ZARB. The higher adsorption in ZARB demonstrates that intercalation modifies the porosity of the material, resulting in a more accessible and interconnected mesoporous network, despite the fact that the H1 hysteresis loop in both materials points to a homogenous pore structure. These modifications show how successfully the intercalation process altered the structural characteristics of ZAL.

The distribution of pore sizes highlights the distinctions between the 2 materials even more. With a tight distribution centered at 18.05 nm, ZAL shows consistent mesopores with little variation. In contrast, ZARB has a wider range with a higher average pore diameter of 20.27 nm, emphasizing the development of more varied pore diameters. Because RB intercalation causes structural disruptions, the wider distribution in ZARB suggests a more heterogeneous porous network. Together, the pore size distribution, isotherm behavior, and textural characteristics validate that RB intercalation is a successful method for improving ZAL's porosity and functionality.

Table 2 The surface Properties of ZAL and ZARB.

Samples	Surface area (m^2g^{-1})	BJH desorption pore volume (cm^3g^{-1})	BJH average pore diameter (nm)
ZAL	5.1897	0.023831	18.0530
ZARB (0.2 M)	14.3001	0.053758	20.2740

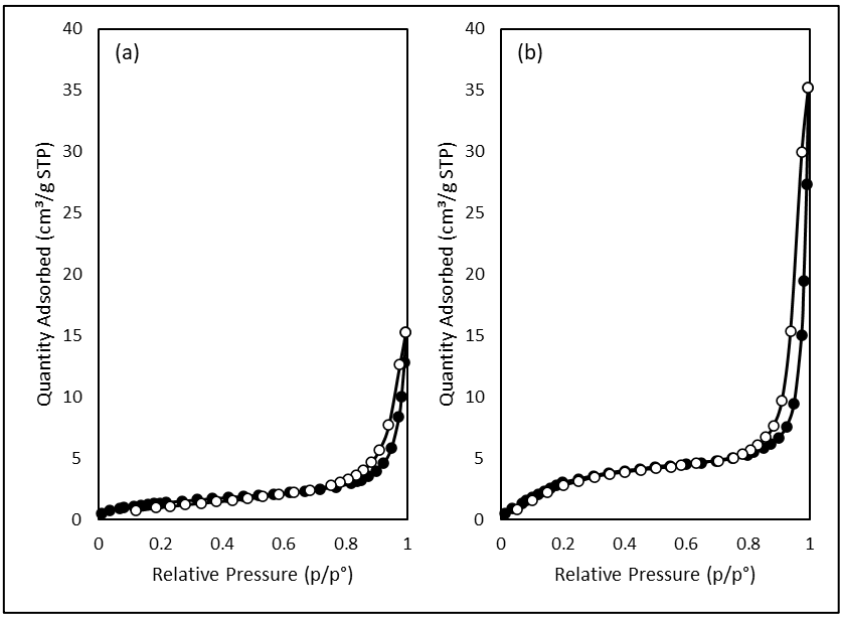

Figure 5 Nitrogen adsorption-desorption isotherm of (a) ZAL and (b) ZARB at concentration 0.2 M.

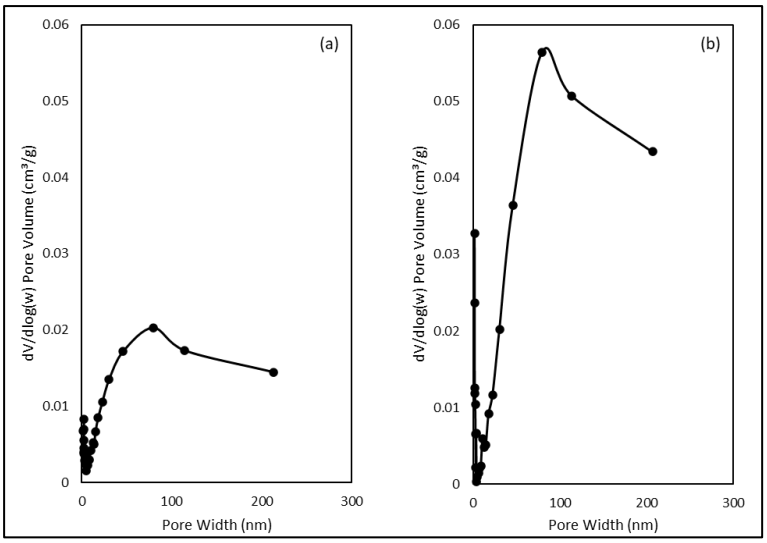

Figure 6 Pore size distribution of (a) ZAL and (b) ZARB at concentration 0.2 M.

Surface morphology - dispersive energy (SEM-EDX)

The surface morphology of the ZAL and ZARB nanocomposites (0.2 M) was observed using SEM coupled with EDX analysis under 10,000 x magnification as shown in **Figure 6**. For the ZAL, the image morphology formed is typical of layered double hydroxide material, which is aggregated hexagonal plate-like with non-uniform particles of different sizes and shapes. After the RB anion had intercalated into the interlayer region of ZAL, the structure changed into an aggregated flaky plate-like materials with higher surface area. In addition, the EDX analysis of intercalated ZAL with RB confirmed the presence of Zn, O, C, Al, N and C as major elements. The percentage of carbon increased from 4.7 %(w/w) of ZAL to 11.5 %(w/w) at concentration (0.2 M). Meanwhile, the percentage of nitrate decreased from 4.1 %(w/w) of ZAL to 1.1 %(w/w) of ZARB at concentration (0.2 M). This is aligned with the enlargement of basal spacing in the PXRD analysis in **Figure 2**, proving the intercalation of RB anion into the layered material.

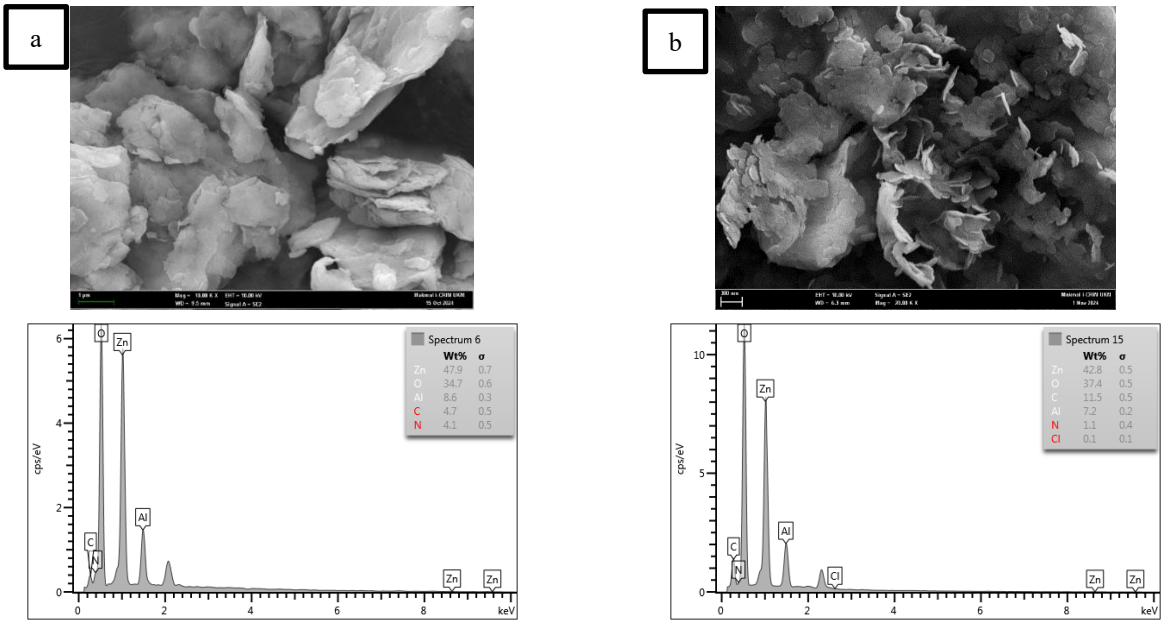

Figure 6 FESEM-EDX images of (a) ZAL and (b) ZARB (0.2 M) at 10,000 x magnification.

Conclusions

This study investigated the intercalation of rhodamine b into Zinc-aluminum layered double hydroxide (ZAL) through co-precipitation method. The results of PXRD, FTIR-ATR, BET and FESEM-EDX analyses confirmed the successful intercalation of the guest anion, RB with ZAL and indicated the success of intercalation between ZAL and RB. Based on the PXRD results, the optimal concentration RB is at 0.2 M with basal expansion of ZARB from 8.9 to 11.0 Å, this result indicates the successfully intercalation of RB anion into ZAL layered. In addition, FTIR-ATR data exhibit further evidence of the characteristic functional groups associated with RB, indicate its effective integration within the layered double hydroxide. The BET results showed increased surface area, BJH desorption pore volume and BJH average pore diameter (nm) of ZARB at concentration 0.2 M. The SEM-EDX data provide the insight of surface morphology ZAL with non-uniform particle of different size and shape, after RB anion intercalated into ZAL layer, the surface morphology ZARB modified to aggregated flaky plate like. The EDX result illustrated the increased of carbon content of ZARB and nitrate content after intercalation occur. The increasing of interlayer distance suggests the effective loading of RB into the layered double hydroxide structure, and from data report the polymorphic transformation during the intercalation process. The synthesized ZARB nanocomposite demonstrates promising potential for application in environmental remediation and sensing technologies. The successful encapsulation of rhodamine B within the LDH framework minimizes its leaching, offering a stable material suitable for dye containment or controlled release systems. Furthermore, the increased surface area and porosity enhance the material's ability to act as an efficient adsorbent or sensing platform for organic pollutants in aqueous environments. Given the structural tunability of LDHs, this approach can be extended to other hazardous dyes or contaminants, making ZARB a multifunctional material for water purification, pollutant detection, and potential photocatalytic applications.

Acknowledgements

The authors gratefully acknowledge the support provided by Universiti Teknologi MARA (UiTM), Malaysia, for the research facilities and institutional assistance throughout the course of this work. This study was funded by the Ministry of Higher Education (MOHE), Malaysia, under the Fundamental Research Grant Scheme (FRGS) (Grant No. FRGS/1/2023/STG05/UITM/02/20).

Declaration of Generative AI in Scientific Writing

The authors acknowledge the use of generative AI tools (e.g., QuillBot and ChatGPT by OpenAI) in the

preparation of this manuscript, specifically for language editing and grammar correction. No content generation or data interpretation was performed by AI. The authors take full responsibility for the content and conclusions of this work.

CRediT Author Statement

Nursyafiqah Jori Roslan- Conceptualization, Methodology, Investigation, Data Curation, Formal Analysis, Lab work and Writing– original draft.

Nur Nadia Dzulkifli- Data curation, Formal analysis,Investigation, Validation, and Visualization

Tengku Shafazila Tengku Saharuddin- Data curation, Formal analysis, Investigation, Validation, and Visualization

Hamizah Mohd Zaki- Data curation, Formal analysis,Investigation, Validation, and Visualization

Syawal Mohd Yusof-Analysis and Instrumentation

Sheikh Ahmad Izaddin Sheikh Ahmad Ghazali- Conceptualization, Methodology, Supervision, Validation, Funding acquisition, and Writing – Review & Editing.

References

[1] MA Al-Hamyd, AS Al-Asadi and MF Al-Mudhaffer. Preparation and characterization of zinc-aluminum layered doubled hydroxide/ graphene nanosheets composite for supercapacitor el ectrode. *Physica E: Low-Dimensional Systems and Nanostructures* 2022; **136**, 115005.

[2] FL Bohari, SAISM Ghazali, NN Dzulkifl, SNA Baharin, I Fatimah and S Poddar. Studies on the intercalation of calcium-aluminium layered double hydroxide-MCPA and its controlled release mechanism as a potential green herbicide. *Open Chemistry* 2023; **20(1)**, 20220291.

[3] M Ebadi, K Buskaran, S Bullo, MZ Hussein, S Fakurazi and G Pastorin. Drug delivery system based on magnetic iron oxide nanoparticles coated with (polyvinyl alcohol-zinc/aluminium-layered double hydroxide-sorafenib). *Alexandria Engineering Journal* 2021; **60(1)**, 733-743.

[4] SAISM Ghazali, SH Sarijo and MZ Hussein. New synthesis of binate herbicide-interleaved anionic clay material: Synthesis, characterization and simultaneous controlled-release properties. *Journal of Porous Materials* 2021; **28**, 495-505.

[5] OMA Halim, NH Mustapha, SNM Fudzi, R Azhar, NIN Zanal, NF Nazua, AH Nordin, MSM Azami, MAM Ishak, W Ismail and Z Ahmad. A review on modified ZnO for the effective degradation of Methylene Blue and Rhodamine B. *Results in Surfaces and Interfaces* 2025; **18**, 100408.

[6] S Iftekhar, ME Kucuk, V Srivastava, E Repo and M Sillanpaa. Application of zinc-aluminium layered double hydroxides for adsorptive removal of phosphate and sulfate: Equilibrium, kinetic and thermodynamic. *Chemosphere* 2018; **209**, 470-479.

[7] SH Jasim and AS Al-Asadi. Graphene oxide/zinc-aluminum double layered hydroxide nanocomposite for hybrid supercapacitor. *Colloids and Surfaces A: Physicochemical and Engineering Aspects* 2025; **709**, 136113.

[8] J Karthikeyan, H Fjellvag, S Bundli and AO Sjastad. Efficient exfoliation of layered double hydroxides; effect of cationic ratio, hydration state, anions and their orientations. *Materials* 2021; **14(2)**, 346.

[9] NASM Sandollah., SAISM Ghazali, WNW Ibrahim and R Rusmin. Adsorption-desorption profile of methylene blue dye on raw and acid activated kaolinite. *Indonesian Journal of Chemistry* 2020; **20(4)**, 755-765.

[10] LBND Farias, GG Carbajal-Arizaga, LGG Sante, L Effting, JACDS Fernandesa and A Bail. Nanoflakes of chloride zinc-iron-aluminum-based layered double hydroxides obtained from industrial waste: A green approach to mass-scale production. *RSC Advances* 2021; **11(29)**, 17760-17768.

[11] A Sharma, S Kumari, S Sharma, T Singh, S Kumar, A Thakur, SK Bhatiam and AK Sharma. Layered double hydroxides: An insight into the role of hydrotalcite-type anionic clays in energy and environmental applications with current progress and recent prospects. *Materials Today Sustainability* 2023; **22**, 100399.

[12] A Yu, Y Song, N Wang, Y Tian and H Chen. Study on the corrosion and self-healing behavior of different anion-intercalated layered double hydroxides coatings on Mg alloy surfaces. *Surfaces and Interfaces* 2025; **56**, 105680.